



HAL
open science

Static stability of manipulator configuration: Influence of the external loading

Alexandr Klimchik, Damien Chablat, Anatol Pashkevich

► To cite this version:

Alexandr Klimchik, Damien Chablat, Anatol Pashkevich. Static stability of manipulator configuration: Influence of the external loading. *European Journal of Mechanics - A/Solids*, 2015, 51, pp.193-203. 10.1016/j.euromechsol.2014.12.010 . hal-01201685

HAL Id: hal-01201685

<https://imt-atlantique.hal.science/hal-01201685v1>

Submitted on 15 Jul 2021

HAL is a multi-disciplinary open access archive for the deposit and dissemination of scientific research documents, whether they are published or not. The documents may come from teaching and research institutions in France or abroad, or from public or private research centers.

L'archive ouverte pluridisciplinaire **HAL**, est destinée au dépôt et à la diffusion de documents scientifiques de niveau recherche, publiés ou non, émanant des établissements d'enseignement et de recherche français ou étrangers, des laboratoires publics ou privés.



Distributed under a Creative Commons Attribution 4.0 International License

Static stability of manipulator configuration: influence of the external loading

Alexandr Klimchik^{a,b,1}, Damien Chablat^{b,c}, Anatol Pashkevich^{a,b},

^a Ecole des Mines de Nantes, 4 rue Alfred-Kastler, Nantes 44307, France

^b Institut de Recherches en Communications et en Cybernétique de Nantes, UMR CNRS 6597, 1 rue de la Noe, 44321 Nantes, France

^c Centre national de la recherche scientifique (CNRS), France

Abstract

The paper deals with the manipulator static stability analysis under the influence of the external loading. It proposes a new technique that allows evaluating both static stability of the end-effector location and static stability of the kinematic chain configuration. This approach extends the classical notion of the manipulator static stability that is completely defined by the properties of the Cartesian stiffness matrix. The advantages of the new approach are illustrated by examples that deal with parallel manipulators and their serial chains. The analysis showed that the manipulator workspace may include elastostatic singularities where the chain configurations become unstable under the influence of external loading.

Keywords:

Parallel robots, stiffness modeling, equilibrium stability, elastostatic singularity.

1 Introduction

Manipulator stiffness modeling under loading is a relatively new research area that is important both for serial and parallel robots (Shan 2002, Su 2003). In general case, loadings may be of different nature and applied to different points/surfaces. To evaluate stiffness properties, several methods can be applied such as Finite Element Analysis, Matrix Structural Analysis and Virtual Joint Modeling (VJM) (Salisbury 1980, Gosselin 1990, Yi 1993, Chen 2002, Xi 2004, Corradini 2004, Chakarov 2004, Alici 2005, Deblaise 2006, Kövecses 2007, Quennouelle 2008, Tyapin 2009, Dumas 2010, Pashkevich 2010, 2011), where the last one is the most attractive in robotic domain since it operates with an extension of the traditional rigid model that is completed by a set of virtual joints (localized springs), which describe elastic properties of the links, joints and actuators.

For *serial manipulators* the VJM approach has been used in the number of works (Salisbury 1980, Gosselin 1990, Chen 2002, Corradini 2004, Alici 2005, Deblaise 2006, Dumas 2010, Pashkevich 2010). The obtained results allows us to compute stiffness matrices both for serial manipulators without passive joints (Salisbury 1980, Chen 2002, Corradini 2004, Alici 2005, Deblaise 2006) and for serial chains of parallel manipulators with passive joints (Pashkevich 2010). However, most of them addressed to the case of small deflections (unloaded mode) (Gosselin 1990, Alici 2005), only limited number of authors consider the case of large deflections (loaded mode) (Salisbury 1980, Deblaise 2006, Dumas 2010, Pashkevich 2010).

For *parallel manipulators*, the stiffness modeling is usually performed for all kinematic chains simultaneously (Gosselin 1990, Wei 2010), using the aggregated elastostatic equilibrium equations (Yi 1993, Quennouelle 2008). In contrast to these works, our approach is based on two-step procedure, which includes stiffness modeling of all kinematic chains *separately* and then *aggregates* them in a unique model. This approach has been already used by several authors (Pashkevich 2010, Xi 2004), but related aggregation technique was reduced to simple summations of the Cartesian stiffness matrices for the kinematic chains and the external loadings applied to their end-points. This corresponds to “pure” parallel architectures where the end-point location of all kinematic chains are aligned and matched at the end-platform reference point. However, in practice, the parallel manipulator architecture is usually quite complex. In particular, the kinematic chains may be attached to different points of the end-platform.

It is obvious that the both external and internal loadings influence on the manipulator equilibrium configuration and, consequently, may modify the stiffness properties. So, they must be undoubtedly taken into account while developing the stiffness model. However, in most of related works the stiffness is evaluated in a quasi-static configuration without external or internal loading. There are very limited number of publications that directly address the case of “large deflections”, where in

¹ Corresponding author. Tel. +33 251 85 83 17; fax. +33 251 85 83 49; E-mail address: alexandr.klimchik@mines-nantes.fr (A. Klimchik).

addition to the conventional “*elastic stiffness*” in the joints it is necessary to take into account the “*geometrical stiffness*” arising due to the change in the manipulator configuration under the load. The most essential results in this area were obtained in (Xi 2004, Tyapin 2009, Dumas 2010, Pashkevich 2010, 2011) where there are presented both some theoretical issues and several case studies for serial and parallel manipulators under end-point loading. Several authors (Quennouelle 2008, Tyapin 2009) addressed the problem of stiffness analysis for the manipulators with internal preloading or antagonistic actuating, but in relevant equations some of the second order kinematic derivatives were neglected. However, no one of them considered auxiliary loading.

This paper contributes to the VJM-based technique and focuses on the static stability analysis of serial and parallel manipulators under external loading. It addressed both static stability of end-platform location and static stability of serial chain configuration. To address these issues, it is proposed a revision of the existing VJM-based stiffness modeling technique that includes development a non-linear stiffness model of the robotic manipulator under essential loading that takes into account the external loading applied to end-effector, preloading in the joints and auxiliary loading applied to intermediate node-points.

2 Problem statement

2.1 Motivation

Traditionally, the configuration static stability of compliant mechanical systems (including manipulators) is defined as *resistance of the end-point location* \mathbf{t} with respect to the “disturbing” effects of an external force \mathbf{F} applied at this point. In such formulation, the static stability is completely defined by the stiffness matrix \mathbf{K}_C that describes the linear relations between the force and deflection deviations $\delta\mathbf{F}$, $\delta\mathbf{t}$ with respect to the values \mathbf{F} , \mathbf{t} .

$$\delta\mathbf{F} = \mathbf{K}_C \cdot \delta\mathbf{t} \tag{1}$$

It is obvious that for the stable location \mathbf{t} the matrix \mathbf{K}_C should be positive definite.

However, in the compliant manipulators with the passive joints, the equilibrium configuration $(\mathbf{q}, \boldsymbol{\theta})$ corresponding to the same end-point location \mathbf{t} cannot be unique (here the vector \mathbf{q} contains passive joint coordinates; the vector $\boldsymbol{\theta}$ collects coordinates of all virtual joints). Moreover, these configurations may be both “stable” and “unstable” and may correspond to different values of potential energy stored in the virtual springs. From this point of view, it is worth to distinguish static stability of the end-point location \mathbf{t} and stability of the corresponding equilibrium configuration of the kinematic chain $(\mathbf{q}, \boldsymbol{\theta})$, which may be defined as a *resistance of the chain shape* with respect to disturbances in redundant kinematic variables. This issue becomes extremely important for the loaded mode, when due to the kinematic redundancy caused by the passive joints and excessive number of virtual springs, small disturbances in $(\mathbf{q}, \boldsymbol{\theta})$ may provoke essential change of current equilibrium configuration leading to the reduction of the potential energy and transition to another equilibrium state, while keeping the same end-point location. Hence, it is necessary to evaluate internal properties of the kinematic chain in the state of the loaded equilibrium that may correspond either to minimum or maximum of the potential energy for a fixed value of \mathbf{t} .

Let us illustrate this notion by the example of three-link chain (Figure 1a), which includes passive joints at both ends and two virtual torsional springs between the links, which insure the “straight” configuration for the unloaded mode. It is assumed that both ends of the chain are fixed by the external geometrical constraints while the internal configuration may change without shifting of the end-points, in accordance with redundant parameter value. It is evident that this chain is loaded, but corresponding value of the force \mathbf{F} depends on particular configuration. Besides, among variety of possible configurations (corresponding to given end-point locations), only equilibrium ones are in the focus of interest.

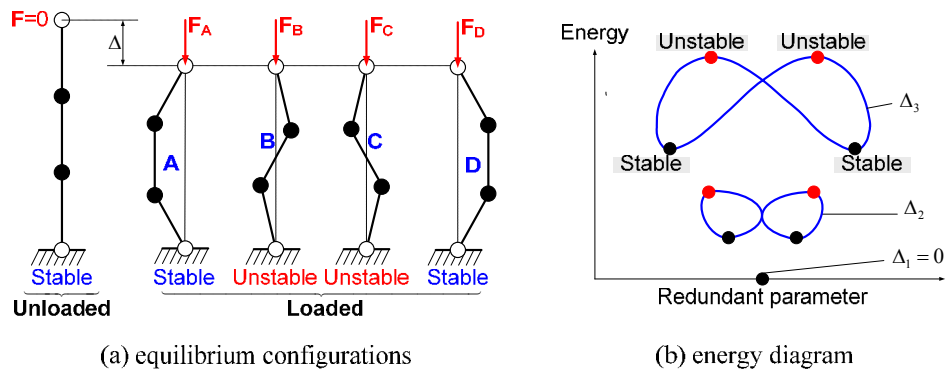


Figure 1 Stable and non-stable configurations of 3-link serial chain and their energy-based interpretation

For this case study, it is convenient to give an energy-based interpretation. The considered kinematic chain has one redundant parameter (rotation angle of any passive joint) and under geometrical constraints may occupy configurations with the different shapes. Relevant relation between the energy stored in the virtual springs and the redundant parameter value is presented in Figure 1b. Due to the physical nature of this chain, for each given end-point displacement Δ , the examined plot presents a continuous closed criss-cross curve that has exactly two minimum and maximum points, that correspond to the stable and unstable equilibriums respectively. Hence, numerical solution of static equilibrium equations may yield both stable and unstable configurations, while in practice only stable ones should be considered. Thus, the criterion that allows us to distinguish stable and unstable configurations of the kinematic chain is required.

Physical meaning of this stability notion (related to the kinematic chain shape) is illustrated in Figure 2, which contains several postures of the same parallel manipulator with exactly the same end-platform location. These postures differ in the shapes of serial kinematic chains that may be treated as internal configuration of the parallel manipulator, which is not "visible" from the end-platform side whose static stability is completely defined by the Cartesian stiffness matrix. In particular, Figure 2a,b present parallel manipulators that include at least one kinematic chain in unstable configuration that cannot be observed in practice but satisfy the general static equilibrium equation. In contrast, Figure 2c shows physically realizable posture of the same manipulator (with exactly the same location of the chain end-points) where, for all kinematic chains, the shapes are stable.

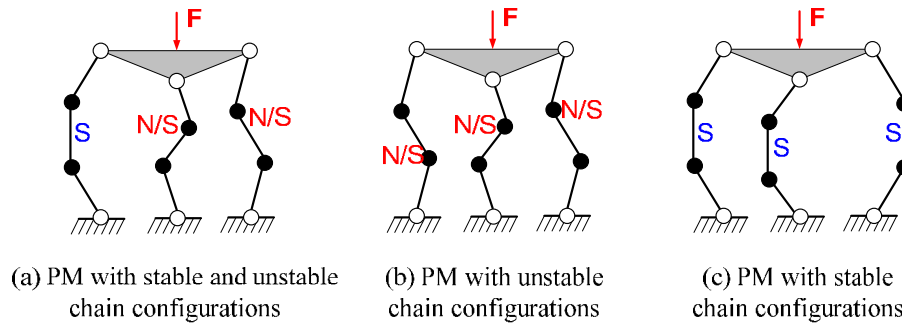


Figure 2 2D parallel manipulators with serial chains in stable and unstable configurations

Hence, full-scale investigation of the stiffness properties of the loaded parallel manipulator must include the stability analysis of the internal kinematic chain configurations that is presented in this paper.

2.2 Basic assumptions and research problems

In order to address the static stability of both end-point location and kinematic chain configuration, it is assumed that parallel manipulator has a strictly parallel structure. In this case, first, it is required to address to the stiffness modeling of serial kinematic chain and then, applying stiffness model aggregation technique, to obtain the stiffness matrix of the parallel manipulator (Klimchik 2012).

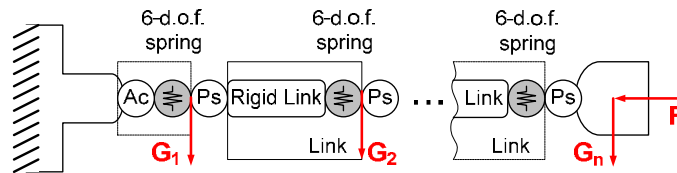


Figure 3 VJM model of kinematic chain with end-point and auxiliary loading

For stiffness modeling of serial kinematic chain let us use VJM model that is presented in Figure 3. This approach provides reasonable trade-off between the computational time and model precision, its recent modification (Pashkevich 2011) allows user to describe elastostatic properties of flexible elements by a general 6 d.o.f. springs. The model parameters can be computed either from the virtual experiment in the CAD environment (Klimchik 2013) or from physical experiments (Dumas 2010). Because of its advantages, the VJM approach is widely used in robotics. Detailed background for this approach has been presented in Pashkevich (2010, 2011).

In this work, it is assumed that the manipulator links and joints can be presented as a sequence of rigid elements and virtual springs that take into account their flexibility. In addition to the end-point loading F , the serial chain has an auxiliary external loadings applied to the internal node points (auxiliary loading). These forces will be denoted as G_j , where $j = 1, \dots, n$ is the node number in the serial chain starting from the fix base. For such kinematic chains it is necessary to introduce the functions defining locations of the nodes

$$\mathbf{t}_j = \mathbf{g}_j(\mathbf{q}, \boldsymbol{\theta}), \quad j = 1, \dots, n \quad (2)$$

where the vector \mathbf{t}_j includes the position and orientation of the j^{th} node; the vector \mathbf{q} contains passive joint coordinates; the vector $\boldsymbol{\theta}$ collects coordinates of all virtual joints, the function $\mathbf{g}_j(\dots)$ defines the geometrical model for the j^{th} node-point.

Using these assumptions and the methodology of VJM method proposed in Pashkevich (2010,2011), the problem of static stability analysis of serial and parallel manipulators under external/internal loading can be split in the following sub-problems: (i) static stability analysis of serial chain configuration that includes computing of the loaded equilibrium configuration, and (ii) static stability of the end-platform location of serial and parallel manipulators.

3 Static stability of kinematic chain configuration under loading

Usually external and internal loadings have affects both end-point location and configuration of serial chain. Therefore, in order to address to the static stability of the kinematic chain configuration; firstly; it is required to compute the loaded equilibrium configuration.

3.1 Static equilibrium

The static equilibrium equations for the manipulators with internal and external loadings (that are applied to both end-effector and intermediate nodes) differ from those used for the end-point loaded manipulator. Using the principle of virtual work it has been proved that the desired static equilibrium equations can be presented as

$$\begin{aligned} \mathbf{J}_\theta^{(G)T} \cdot \mathbf{G} + \mathbf{J}_\theta^T \cdot \mathbf{F} &= \mathbf{K}_\theta \cdot (\boldsymbol{\theta} - \boldsymbol{\theta}^0) \\ \mathbf{J}_q^{(G)T} \cdot \mathbf{G} + \mathbf{J}_q^T \cdot \mathbf{F} &= \mathbf{0} \end{aligned} \quad (3)$$

where the matrices $\mathbf{J}_\theta^{(G)}$, $\mathbf{J}_q^{(G)}$ aggregate Jacobians for the node points with respect to the virtual and passive joint coordinates, \mathbf{G} collects the vectors of auxiliary loadings, \mathbf{J}_θ , \mathbf{J}_q are Jacobians for the end-effector with respect to the virtual and passive joint coordinates respectively, \mathbf{F} is the external loading applied to the end-effector, the matrix \mathbf{K}_θ defines elastostatic properties of the serial chain, $\boldsymbol{\theta}$ is the vector of virtual joint coordinates whose unloaded values are defined by $\boldsymbol{\theta}^0$. The matrices \mathbf{J}_θ , \mathbf{J}_q , $\mathbf{J}_\theta^{(G)}$, $\mathbf{J}_q^{(G)}$, \mathbf{G} are defined in the following way

$$\mathbf{J}_\theta = \mathbf{J}_\theta^{(n)}; \quad \mathbf{J}_q = \mathbf{J}_q^{(n)}; \quad \mathbf{J}_\theta^{(G)} = [\mathbf{J}_\theta^{(1)T} \dots \mathbf{J}_\theta^{(n)T}]^T; \quad \mathbf{J}_q^{(G)} = [\mathbf{J}_q^{(1)T} \dots \mathbf{J}_q^{(n)T}]^T; \quad \mathbf{G} = [\mathbf{G}_1^T \dots \mathbf{G}_n^T]^T \quad (4)$$

where Jacobians with respect to the virtual and passive joint coordinates respectively are computed as

$$\mathbf{J}_\theta^{(j)} = \frac{\partial}{\partial \boldsymbol{\theta}} \mathbf{g}_j(\mathbf{q}, \boldsymbol{\theta}); \quad \mathbf{J}_q^{(j)} = \frac{\partial}{\partial \mathbf{q}} \mathbf{g}_j(\mathbf{q}, \boldsymbol{\theta}) \quad (5)$$

To obtain a relation between the external loading \mathbf{F} and internal coordinates of the kinematic chain $(\mathbf{q}, \boldsymbol{\theta})$ corresponding to the static equilibrium, Eq. (3) should be solved either for given values of \mathbf{F} or for different given values of \mathbf{t} . In Pashkevich (2011) these problems were referred to as the original and the dual ones respectively, but the dual problem was discovered to be the most convenient from computational point of view. Hence, let us solve static equilibrium equations with respect to manipulator configuration $(\mathbf{q}, \boldsymbol{\theta})$ and external loading \mathbf{F} for given end-effector position $\mathbf{t} = \mathbf{g}(\mathbf{q}, \boldsymbol{\theta})$ and function of auxiliary-loadings $\mathbf{G}(\mathbf{q}, \boldsymbol{\theta})$

Since usually this system has no analytical solution, iterative numerical technique can be applied. For this purpose, the kinematic equations may be linearized in the neighborhood of the current configuration $(\mathbf{q}_i, \boldsymbol{\theta}_i)$

$$\mathbf{t}_{i+1} = \mathbf{g}(\mathbf{q}_i, \boldsymbol{\theta}_i) + \mathbf{J}_\theta(\mathbf{q}_i, \boldsymbol{\theta}_i) \cdot (\boldsymbol{\theta}_{i+1} - \boldsymbol{\theta}_i) + \mathbf{J}_q(\mathbf{q}_i, \boldsymbol{\theta}_i) \cdot (\mathbf{q}_{i+1} - \mathbf{q}_i); \quad (6)$$

where the subscript "i" denotes the iteration number (i.e. subscript "i" indicates previous iteration and "i+1" corresponds to the next one) and the changes in Jacobians $\mathbf{J}_\theta^{(G)}$, \mathbf{J}_θ , $\mathbf{J}_q^{(G)}$, \mathbf{J}_q and variation of the auxiliary loadings $\mathbf{G}(\mathbf{q}, \boldsymbol{\theta})$ from iteration to iteration are assumed to be negligible. Correspondingly, the static equilibrium equations in the neighborhood of $(\mathbf{q}_i, \boldsymbol{\theta}_i)$ may be rewritten as

$$\begin{aligned} \mathbf{J}_\theta^{(G)T} \cdot \mathbf{G} + \mathbf{J}_\theta^T \cdot \mathbf{F}_{i+1} &= \mathbf{K}_\theta \cdot (\boldsymbol{\theta}_{i+1} - \boldsymbol{\theta}^0) \\ \mathbf{J}_q^{(G)T} \cdot \mathbf{G} + \mathbf{J}_q^T \cdot \mathbf{F}_{i+1} &= \mathbf{0} \end{aligned} \quad (7)$$

Thus, combining Eq. (6) and (7), the iterative algorithm for computing the static equilibrium configuration for given end-effector location can be presented as

$$\begin{bmatrix} \mathbf{F}_{i+1} \\ \mathbf{q}_{i+1} \\ \boldsymbol{\theta}_{i+1} \end{bmatrix} = \begin{bmatrix} \mathbf{0} & \mathbf{J}_q & \mathbf{J}_\theta \\ \mathbf{J}_q^T & \mathbf{0} & \mathbf{0} \\ \mathbf{J}_\theta^T & \mathbf{0} & -\mathbf{K}_\theta \end{bmatrix}^{-1} \begin{bmatrix} \mathbf{t}_{i+1} - \mathbf{g}(\mathbf{q}_i, \boldsymbol{\theta}_i) + \mathbf{J}_\theta \cdot \boldsymbol{\theta}_i + \mathbf{J}_q \cdot \mathbf{q}_i \\ -\mathbf{J}_q^{(G)T} \cdot \mathbf{G}_i \\ -\mathbf{J}_\theta^{(G)T} \cdot \mathbf{G}_i - \mathbf{K}_\theta \cdot \boldsymbol{\theta}_i \end{bmatrix} \quad (8)$$

where $\mathbf{G}_i = \mathbf{G}(\mathbf{q}_i, \boldsymbol{\theta}_i)$.

The proposed algorithm allows us to compute the static equilibrium configuration for the serial chains with passive joints and all types of loadings (internal preloading, external loadings applied to any point of the manipulator and loading from the technological process). The convergence properties of this algorithm are similar to one presented in Pashkevich (2011). Also, it can be modified to solve the problem of computing the equilibrium configuration corresponding to given external loading.

3.2 Stability criterion

To evaluate stability of the static equilibrium configuration $(\mathbf{q}, \boldsymbol{\theta})$ of a separate kinematic chain, let us assume that the end-point is fixed at the point $\mathbf{t} = (\mathbf{p}, \boldsymbol{\varphi})^T$ corresponding to the external load \mathbf{F} , but the joint coordinates are given small virtual displacements $\delta\mathbf{q}$, $\delta\boldsymbol{\theta}$ satisfying the geometrical constraint (2), i.e.

$$\mathbf{t} = \mathbf{g}(\mathbf{q}, \boldsymbol{\theta}); \quad \mathbf{t} = \mathbf{g}(\mathbf{q} + \delta\mathbf{q}, \boldsymbol{\theta} + \delta\boldsymbol{\theta}) \quad (9)$$

For these assumptions, let us compute the total virtual work in the joints that must be positive for a stable equilibrium and negative for an unstable one. To achieve the virtual configuration $(\mathbf{q} + \delta\mathbf{q}, \boldsymbol{\theta} + \delta\boldsymbol{\theta})$ and restore the equilibrium conditions, each joint must include a virtual spring that generates the generalized forces/torques $\delta\boldsymbol{\tau}_q$, $\delta\boldsymbol{\tau}_\theta$ which satisfies the equations:

$$\mathbf{J}_\theta^T \cdot \mathbf{F} = \mathbf{K}_\theta \cdot (\boldsymbol{\theta} - \boldsymbol{\theta}_0); \quad \mathbf{J}_q^T \cdot \mathbf{F} = 0 \quad (10)$$

$$\begin{aligned} (\mathbf{J}_\theta + \delta\mathbf{J}_\theta)^T \cdot \mathbf{F} &= \mathbf{K}_\theta \cdot (\boldsymbol{\theta} - \boldsymbol{\theta}_0 + \delta\boldsymbol{\theta}) + \delta\boldsymbol{\tau}_\theta \\ (\mathbf{J}_q + \delta\mathbf{J}_q)^T \cdot \mathbf{F} &= \delta\boldsymbol{\tau}_q \end{aligned} \quad (11)$$

where the matrices $\delta\mathbf{J}_\theta$, $\delta\mathbf{J}_q$ define deviations in the Jacobian matrices caused by the increment of virtual joint displacements $\delta\boldsymbol{\theta}$ and $\delta\mathbf{q}$, the vectors $\delta\boldsymbol{\tau}_\theta$, $\delta\boldsymbol{\tau}_q$ describe relevant changes in the torque of virtual and passive joints respectively.

After relevant transformations, the virtual torques may be expressed as

$$\delta\boldsymbol{\tau}_\theta = \delta(\mathbf{J}_\theta^T \cdot \mathbf{F}) - \mathbf{K}_\theta \cdot \delta\boldsymbol{\theta}; \quad \delta\boldsymbol{\tau}_q = \delta(\mathbf{J}_q^T \cdot \mathbf{F}) \quad (12)$$

where $\delta(\dots)$ denotes the differential with respect to $\delta\mathbf{q}$, $\delta\boldsymbol{\theta}$ that may be expanded via Hessians of the scalar function $\Psi = \mathbf{g}(\mathbf{q}, \boldsymbol{\theta})^T \cdot \mathbf{F}$:

$$\begin{aligned} \delta(\mathbf{J}_\theta^T \cdot \mathbf{F}) &= \mathbf{H}_{\theta q}^F \cdot \delta\mathbf{q} + \mathbf{H}_{\theta\theta}^F \cdot \delta\boldsymbol{\theta} \\ \delta(\mathbf{J}_q^T \cdot \mathbf{F}) &= \mathbf{H}_{q q}^F \cdot \delta\mathbf{q} + \mathbf{H}_{q\theta}^F \cdot \delta\boldsymbol{\theta} \end{aligned} \quad (13)$$

provided that

$$\mathbf{H}_{q q}^F = \partial^2 \Psi / \partial \mathbf{q}^2; \quad \mathbf{H}_{\theta\theta}^F = \partial^2 \Psi / \partial \boldsymbol{\theta}^2; \quad \mathbf{H}_{q\theta}^F = \mathbf{H}_{\theta q}^{F T} = \partial^2 \Psi / \partial \mathbf{q} \partial \boldsymbol{\theta} \quad (14)$$

Further, taking into account that the virtual displacement from $(\mathbf{q}, \boldsymbol{\theta})$ to $(\mathbf{q} + \delta\mathbf{q}, \boldsymbol{\theta} + \delta\boldsymbol{\theta})$ leads to a gradual change of the torques in the virtual joints from $(\mathbf{0}, \mathbf{0})$ to $(\delta\boldsymbol{\tau}_q, \delta\boldsymbol{\tau}_\theta)$, the virtual work may be computed as a half of the corresponding scalar products

$$\delta W = -\frac{1}{2} (\delta\boldsymbol{\tau}_\theta^T \cdot \delta\boldsymbol{\theta} + \delta\boldsymbol{\tau}_q^T \cdot \delta\mathbf{q}) \quad (15)$$

where the minus sign takes into account the adopted conventions for the positive directions of the forces and displacements. Hence, after appropriate substitutions and transformations to the matrix form, the desired stability condition may be written as

$$\delta W = -\frac{1}{2} \begin{bmatrix} \delta\boldsymbol{\theta}^T & \delta\mathbf{q}^T \end{bmatrix} \cdot \begin{bmatrix} \mathbf{H}_{\theta\theta}^F - \mathbf{K}_\theta & \mathbf{H}_{q\theta}^F \\ \mathbf{H}_{\theta q}^F & \mathbf{H}_{q q}^F \end{bmatrix} \cdot \begin{bmatrix} \delta\boldsymbol{\theta} \\ \delta\mathbf{q} \end{bmatrix} > 0 \quad (16)$$

where $\delta\mathbf{q}$ and $\delta\boldsymbol{\theta}$ must satisfy (9).

In order to take into account the relation between $\delta\mathbf{q}$ and $\delta\boldsymbol{\theta}$ that is imposed by (9), let us apply the first-order expansion of the function $\mathbf{g}(\boldsymbol{\theta}, \mathbf{q})$ that yields the following linear relation

$$\begin{bmatrix} \mathbf{J}_\theta & \mathbf{J}_q \end{bmatrix} \cdot \begin{bmatrix} \delta\boldsymbol{\theta} \\ \delta\mathbf{q} \end{bmatrix} = \mathbf{0} \quad (17)$$

Then, applying the SVD-factorization of $[\mathbf{J}_\theta, \mathbf{J}_q]$

$$\begin{bmatrix} \mathbf{J}_\theta & \mathbf{J}_q \end{bmatrix} = \begin{bmatrix} \mathbf{U}_\theta & \mathbf{U}_q \end{bmatrix} \cdot \begin{bmatrix} \mathbf{S}_r & \\ & \mathbf{0} \end{bmatrix} \cdot \begin{bmatrix} \mathbf{V}_\theta^T \\ \mathbf{V}_q^T \end{bmatrix} \quad (18)$$

where $\mathbf{U} = [\mathbf{U}_\theta, \mathbf{U}_q]$ and $\mathbf{V} = [\mathbf{V}_\theta, \mathbf{V}_q]$ are orthogonal matrices, the second factor \mathbf{S}_r is diagonal matrix containing r positive real numbers $\sigma_1, \sigma_2, \dots, \sigma_r$ in descending order; and extracting from $\mathbf{V}_\theta, \mathbf{V}_q$ the sub-matrices $\mathbf{V}_\theta^o, \mathbf{V}_q^o$ corresponding to zero singular values, a relevant null-space of the system (17) may be presented as

$$\delta\boldsymbol{\theta} = \mathbf{V}_\theta^o \cdot \delta\boldsymbol{\mu}; \quad \delta\mathbf{q} = \mathbf{V}_q^o \cdot \delta\boldsymbol{\mu} \quad (19)$$

where $\delta\boldsymbol{\mu}$ is the arbitrary vector of the appropriate dimension (equal to the rank-deficiency of the integrated Jacobian $[\mathbf{J}_\theta, \mathbf{J}_q]$). Hence, changing of the potential energy δW because of variation of the redundant variables $\delta\boldsymbol{\mu}$ (16) may be rewritten as

$$\delta W = -\frac{1}{2} \delta\boldsymbol{\mu}^T \cdot \begin{bmatrix} \mathbf{V}_\theta^o \\ \mathbf{V}_q^o \end{bmatrix}^T \cdot \begin{bmatrix} \mathbf{H}_{\theta\theta}^F - \mathbf{K}_\theta & \mathbf{H}_{q\theta}^F \\ \mathbf{H}_{\theta q}^F & \mathbf{H}_{qq}^F \end{bmatrix} \cdot \begin{bmatrix} \mathbf{V}_\theta^o \\ \mathbf{V}_q^o \end{bmatrix} \cdot \delta\boldsymbol{\mu} > 0 \quad (20)$$

that must be satisfied for all arbitrary non-zero $\delta\boldsymbol{\mu}$. Hence, the considered static equilibrium configuration $(\mathbf{q}, \boldsymbol{\theta})$ is stable if (and only if) the matrix

$$\mathbf{S}_c = \begin{bmatrix} \mathbf{V}_\theta^o \\ \mathbf{V}_q^o \end{bmatrix}^T \cdot \begin{bmatrix} \mathbf{H}_{\theta\theta}^F - \mathbf{K}_\theta & \mathbf{H}_{q\theta}^F \\ \mathbf{H}_{\theta q}^F & \mathbf{H}_{qq}^F \end{bmatrix} \cdot \begin{bmatrix} \mathbf{V}_\theta^o \\ \mathbf{V}_q^o \end{bmatrix} < 0 \quad (21)$$

is negative-definite. It is worth mentioning that the obtained result is in a good agreement with the previous studies (Chen 2002), where (for the manipulators without passive joints) the stiffness properties were defined by the matrix $\mathbf{K}_\theta - \mathbf{H}_{\theta\theta}^F$ that evidently must be positive-definite for the stable configurations. It should be noted that components of the matrix \mathbf{S}_c depend on elastostatic and geometrical parameters of the serial chain as well as its configuration and the external loading.

Thus, the proposed static stability analysis technique for serial chain with the passive joints and related matrix stability criterion for the kinematic chain configuration allow us to estimate the stability of the serial chain configuration under the external loading in the case of single and multiple equilibriums.

4 Static stability of the end-platform location under external loading

Similar in the structural mechanics stability of the robot end-platform location is defined by the Cartesian stiffness matrix. However, stiffness matrices of serial and parallel manipulators are computed in a different manner (here, to compute stiffness matrix of parallel manipulator it is required to have stiffness matrices of all its serial chains). Let us address them sequentially.

4.1 Cartesian stiffness matrix of a serial kinematic chain

Following the virtual work technique and using static equilibrium equations (3), force deflection relations for the considered serial chain can be expressed as

$$\begin{bmatrix} \delta\mathbf{t} \\ \mathbf{0} \\ \mathbf{0} \end{bmatrix} = \begin{bmatrix} \mathbf{0} & \mathbf{J}_q & \mathbf{J}_\theta \\ \mathbf{J}_q^T & \mathbf{H}_{qq} & \mathbf{H}_{q\theta} \\ \mathbf{J}_\theta^T & \mathbf{H}_{\theta q} & -\mathbf{K}_\theta + \mathbf{H}_{\theta\theta} \end{bmatrix} \cdot \begin{bmatrix} \delta\mathbf{F} \\ \delta\mathbf{q} \\ \delta\boldsymbol{\theta} \end{bmatrix} \quad (22)$$

where Hessians can be computed as

$$\mathbf{H}_{v_1 v_2} = \mathbf{H}_{v_1 v_2}^{(F)} + \mathbf{H}_{v_1 v_2}^{(G)} + \mathbf{J}_{v_1}^{(G)T} \cdot \frac{\partial}{\partial \mathbf{v}_2} \mathbf{G} \quad (23)$$

where $(\mathbf{v}_1, \mathbf{v}_2) \in \{(\mathbf{q}, \mathbf{q}), (\mathbf{q}, \boldsymbol{\theta}), (\boldsymbol{\theta}, \mathbf{q}), (\boldsymbol{\theta}, \boldsymbol{\theta})\}$ and

$$\mathbf{H}_{\mathbf{v}_1 \mathbf{v}_2}^{(G)} = \sum_{j=1}^n \frac{\partial^2}{\partial \mathbf{v}_1 \partial \mathbf{v}_2} (\mathbf{g}_j^T \cdot \mathbf{G}_j); \quad \mathbf{H}_{\mathbf{v}_1 \mathbf{v}_2}^{(F)} = \sum_{j=1}^n \frac{\partial^2}{\partial \mathbf{v}_1 \partial \mathbf{v}_2} (\mathbf{g}_j^T \cdot \mathbf{F}); \quad (24)$$

Hence, the desired stiffness matrices can be computed via the matrix inversion

$$\begin{bmatrix} \mathbf{K}_C & * & * \\ * & * & * \\ * & * & * \end{bmatrix} = \begin{bmatrix} \mathbf{0} & \mathbf{J}_q & \mathbf{J}_\theta \\ \mathbf{J}_q^T & \mathbf{H}_{qq} & \mathbf{H}_{q\theta} \\ \mathbf{J}_\theta^T & \mathbf{H}_{\theta q} & -\mathbf{K}_\theta + \mathbf{H}_{\theta\theta} \end{bmatrix}^{-1} \quad (25)$$

Further, using several analytical transformations and applying the block matrix inversion technique of Frobenius (Gantmacher 1959), the Cartesian stiffness matrix can be compute as

$$\mathbf{K}_C = \mathbf{K}_C^{0(F)} + \mathbf{K}_C^{0(F)} \cdot \mathbf{k}_q^F \cdot \mathbf{K}_C^{0(F)} \quad (26)$$

where the first term $\mathbf{K}_C^{0(F)} = (\mathbf{J}_\theta \cdot \mathbf{k}_\theta^F \cdot \mathbf{J}_\theta^T)^{-1}$ exactly corresponds to the classical formula defining stiffness of the kinematic chain without passive joints in the loaded mode, (Alici 2005), and the second term take into account influence of passive joints via matrix \mathbf{k}_q^F

$$\mathbf{k}_q^F = \mathbf{J}_q^F \cdot (\mathbf{H}_{qq} + \mathbf{H}_{q\theta} \cdot \mathbf{k}_\theta^F \cdot \mathbf{H}_{\theta q} - \mathbf{J}_q^{FT} \cdot \mathbf{K}_C^{0(F)} \cdot \mathbf{J}_q^F)^{-1} \cdot \mathbf{J}_q^{FT} \quad (27)$$

here \mathbf{k}_θ^F denotes the modified joint compliance matrix $\mathbf{k}_\theta^F = (\mathbf{K}_\theta - \mathbf{H}_{\theta\theta})^{-1}$ and matrix \mathbf{J}_q^F denotes the modified Jacobian with respect to passive joints $\mathbf{J}_q^F = (\mathbf{J}_q + \mathbf{J}_\theta \cdot \mathbf{k}_\theta^F \cdot \mathbf{H}_{\theta q})$.

Thus, the Cartesian stiffness matrix obtained using Eq. (26) allows us to analyze the static stability of the serial manipulator (or kinematic chain) end-point location under external/internal loadings. If this stiffness matrix is positive definite the end-point location is stable, and if it is rank-deficient (negative definite) it is possible to move end-point location without additional efforts.

4.2 Cartesian stiffness matrix of parallel manipulator

Let us assume that a parallel manipulator may be presented as a strictly parallel system of the actuated serial legs connecting the base and the end-platform (Merlet 2008). Using the methodology described in previous sections and applying it to each leg, there can be computed a set of m Cartesian stiffness matrices $\mathbf{K}_C^{(i)}$ expressed with respect to the same coordinate system but corresponding to different platform points (Figure 4). If initially the chain stiffness matrices were computed in local coordinate systems, their transformation is performed in a standard way (Angeles 2007).

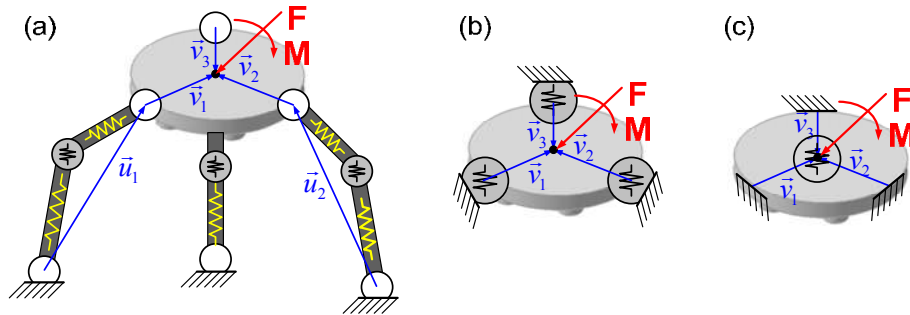


Figure 4 Typical parallel manipulator (a) and transformation of its VJM models (b, c)

After such extension, an equivalent stiffness matrix of the leg may be expressed using relevant expression for a usual serial chain, i.e. as $\mathbf{J}_v^{(i)-T} \cdot \mathbf{K}_C^{(i)} \cdot \mathbf{J}_v^{(i)}$, where the Jacobian $\mathbf{J}_v^{(i)}$ defines differential relation between the coordinates of the i -th virtual spring and the reference frame of the end-platform. Hence, the final expression for the stiffness matrix of the considered parallel manipulator can be written as

$$\mathbf{K}_C^{(m)} = \sum_{i=1}^m \left(\mathbf{J}_v^{(i)-T} \cdot \mathbf{K}_C^{(i)} \cdot \mathbf{J}_v^{(i)} \right) \quad (28)$$

where m is the number of serial kinematic chains in the manipulator architecture.

As a result, Eq. (28) allows us to compute the Cartesian stiffness matrix for the parallel manipulator based on the stiffness matrices for serial chains and transformation Jacobians $\mathbf{J}_v^{(i)}$, which define geometrical mapping between the end-points of serial chains and the reference point frame (the end-effector). Hence, the axes of all virtual springs are parallel to the axes x, y, z of this system. This allows us to evaluate Jacobians $\mathbf{J}_v^{(i)}$ and their inverses from the geometry of end-platform analytically

$$\mathbf{J}_v^{(i)} = \begin{bmatrix} \mathbf{I}_3 & (\mathbf{v}_i \times) \\ \mathbf{0} & \mathbf{I}_3 \end{bmatrix}_{6 \times 6}, \quad \mathbf{J}_v^{(i-1)} = \begin{bmatrix} \mathbf{I}_3 & -(\mathbf{v}_i \times) \\ \mathbf{0} & \mathbf{I}_3 \end{bmatrix}_{6 \times 6} \quad (29)$$

where \mathbf{I}_3 is 3×3 identity matrix, and $(\mathbf{v} \times)$ is a skew-symmetric matrix corresponding to the vector \mathbf{v} , that defines the end-platform location with respect to the end-point of kinematic chain.

It should be mentioned that the proposed approach is also able to take into account geometry of end-platform and its connection with kinematic chains in an explicit form. Finally, using results of Eq. (28) it is possible to analyze the static stability of the end-effector location of the parallel manipulator under external loading.

5 Application examples

5.1 Stiffness analysis for serial chain with 1D-springs

Let us illustrate the efficiency of the developed techniques on the example of 3-link kinematic chain with rigid links and two virtual springs between them. It is assumed that both ends of the chain are fixed with rotational passive joints, all link lengths are equal to l and the stiffness coefficient of both springs are equal to K_θ . The end-point location of considered serial chain can be expressed using geometrical model as

$$\begin{aligned} x &= l \cdot \cos(q) + l \cdot \sin(q + \theta_1) + l \cdot \cos(q + \theta_1 + \theta_2) \\ y &= l \cdot \sin(q) + l \cdot \sin(q + \theta_1) + l \cdot \sin(q + \theta_1 + \theta_2) \\ \varphi &= q + \theta_1 + \theta_2 \end{aligned} \quad (30)$$

where coordinates x, y define end-point location and angle φ defines its orientation, q and (θ_1, θ_2) are passive and virtual joint coordinates respectively that define the serial chain configuration (see Figure 5 for details). It is assumed that external loading is applied along x -direction only and the manipulator end-point can move along x -axis only. So external loading \mathbf{F} can be presented as $\mathbf{F} = [F \ 0]^T$ where F is applied external loading along x -axis.

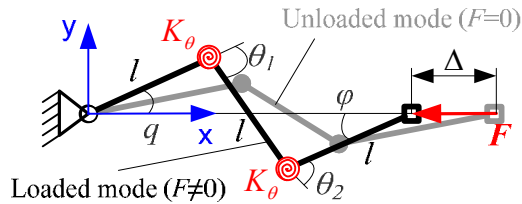


Figure 5 Kinematic chain with flexible actuators and rigid links under external loading

Assuming that the initial values of the actuating coordinates (i.e. before the loading) are denoted as θ_1^0, θ_2^0 , the potential energy stored in the virtual springs may be expressed as the following function of the redundant variable

$$E(q) = \frac{1}{2} K_\theta (\theta_1(q) - \theta_1^0)^2 + \frac{1}{2} K_\theta (\theta_2(q) - \theta_2^0)^2 \quad (31)$$

where K_θ is the stiffness coefficient, and θ_1, θ_2 are computed via the inverse kinematics. Using these equations, the desired equilibriums may be computed from the extremum of $E(q)$. In particular, stable equilibriums correspond to minima of this function, and unstable ones correspond to maxima.

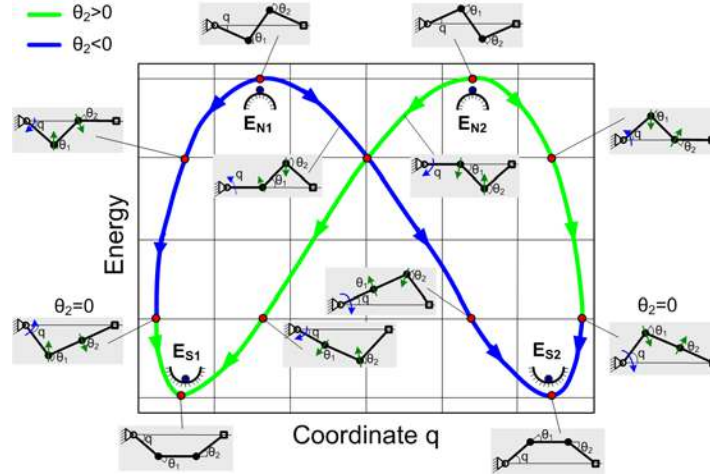


Figure 6 Energy diagram for 3-link serial chain

To illustrate this approach, Figure 6 presents a case study for the initial S-configuration ($q^0 = 0^\circ$, $\theta_1^0 = 0^\circ$ and $\theta_2^0 = 0^\circ$). It allows comparing 12 different shapes of the deformed chain and selecting the best /worst cases with respect to the energy. As it follows from these results, here there are two symmetrical maximum and two minimum, i.e. two stable and two unstable equilibriums. Besides, the stable equilibriums correspond to Π -shaped deformed postures, and the unstable ones correspond to Z-shaped postures, as it is shown in Figure 7.

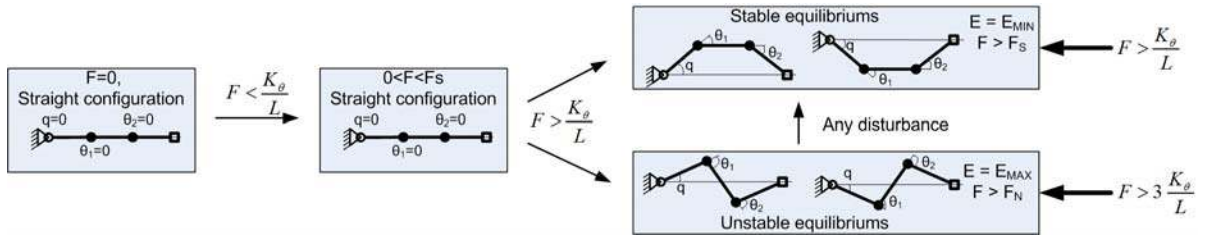


Figure 7 Evolution of the S-configuration under loading

If the assumption concerning small values of δ is released, analytical solutions for the non-trivial equilibriums may be still derived. In particular, for the stable equilibrium, one can get

$$F_S(\Delta) = \frac{K_\theta}{L} \cdot \frac{\varphi}{\sin \varphi} \quad (32)$$

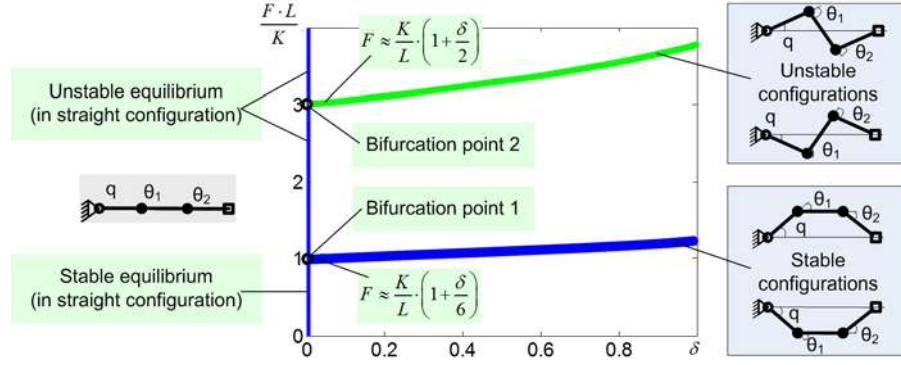
where $\varphi = \pm \arccos(1 - \Delta/2)$. For the unstable equilibrium similar equation may be written as

$$F_N(\Delta) = \frac{K_\theta}{L} \cdot \frac{\cos(q+\theta) + 2 \cdot \cos q}{\sin \theta} \cdot \theta \quad (33)$$

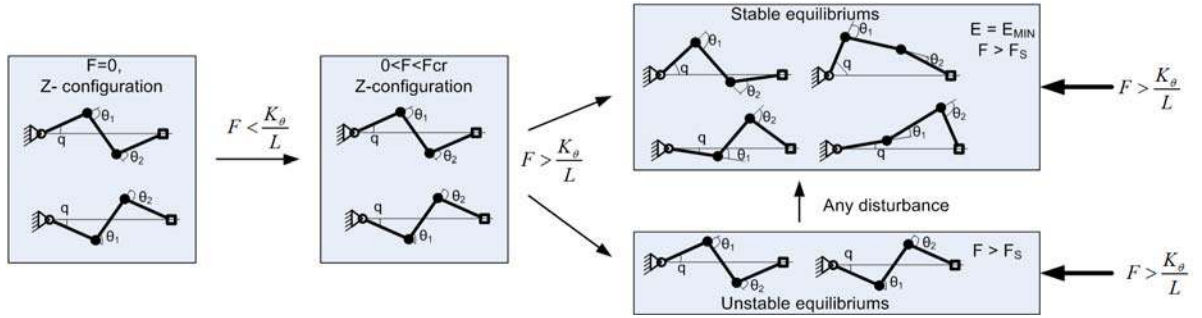
where

$$q = \pm \arccos\left(\frac{12 - 6\Delta + \Delta^2}{12 - 4\Delta}\right); \quad \theta = \mp \arccos\left(1 - \frac{3\Delta}{2} + \frac{\Delta^2}{4}\right) \quad (34)$$

Corresponding plots with the bifurcation are presented in Figure 8. The interpretation of this plot is similar to the axial compression of a straight column, which is a classical example in the strength of materials. It should be noted, that the developed numerical algorithm exactly produces the curve corresponding to the stable equilibrium.


Figure 8 Force-deflection relations for S-configuration

However, for Z-configuration that corresponds to the unloaded zig-zag shape, the stiffness behavior demonstrates the buckling that leads to sudden transformation from a symmetrical to a non-symmetrical posture as shown in Figure 9. Here, there exist two stable equilibriums that differ in the values of the potential energy.


Figure 9 Evolution of the Z-configuration under loading

In order to analyze static stability of different configurations let us define Jacobians and Hessian matrices. For the considered serial chain Jacobians can be expressed as

$$\mathbf{J}_0 = l \begin{bmatrix} -\sin(q + \theta_1) - \sin(q + \theta_1 + \theta_2) & -\sin(q + \theta_1 + \theta_2) \\ \cos(q + \theta_1) + \cos(q + \theta_1 + \theta_2) & \cos(q + \theta_1 + \theta_2) \end{bmatrix} \quad (35)$$

and

$$\mathbf{J}_q = l \begin{bmatrix} -\sin(q) - \sin(q + \theta_1) - \sin(q + \theta_1 + \theta_2) \\ \cos(q) + \cos(q + \theta_1) + \cos(q + \theta_1 + \theta_2) \end{bmatrix} \quad (36)$$

and Hessians as

$$\mathbf{H}_{00} = -F \cdot l \begin{bmatrix} \cos(q + \theta_1) + \cos(q + \theta_1 + \theta_2) & \cos(q + \theta_1 + \theta_2) \\ \cos(q + \theta_1 + \theta_2) & \cos(q + \theta_1 + \theta_2) \end{bmatrix} \quad (37)$$

$$\mathbf{H}_{0q} = -F \cdot l \begin{bmatrix} \cos(q + \theta_1) + \cos(q + \theta_1 + \theta_2) \\ \cos(q + \theta_1 + \theta_2) \end{bmatrix} \quad (38)$$

$$\mathbf{H}_{q0} = -F \cdot l \begin{bmatrix} \cos(q + \theta_1) + \cos(q + \theta_1 + \theta_2) \\ \cos(q + \theta_1 + \theta_2) \end{bmatrix}^T \quad (39)$$

$$\mathbf{H}_{qq} = -F \cdot l [\cos(q) + \cos(q + \theta_1) + \cos(q + \theta_1 + \theta_2)] \quad (40)$$

The eigenvectors for the matrix \mathbf{V} that is required in (21) can be obtained from the matrix $\mathbf{J}^T \cdot \mathbf{J}$, where $\mathbf{J} = [\mathbf{J}_0, \mathbf{J}_q]$, which for the considered serial chain can be computed from

$$\mathbf{J}^T \cdot \mathbf{J} = -F_x^2 \cdot l^2 \cdot \begin{bmatrix} 3 & 2 + \cos(\theta_2) & 2 + \cos(\theta_2) \\ 2 + \cos(\theta_2) & 2 & 1 + \cos(\theta_2) \\ 2 + \cos(\theta_2) & 1 + \cos(\theta_2) & 1 \end{bmatrix} \quad (41)$$

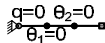
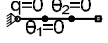
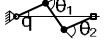
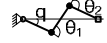

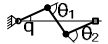
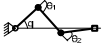
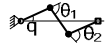
In order to obtain eigenvalues of (41), it is required to solve the third order equation

$$\lambda^3 - 6\lambda^2 - \lambda \cdot (6\cos(\theta_2) - 2) - 3\cos^3(\theta_2) - 4\cos^2(\theta_2) + 2\cos(\theta_2) + 1 = 0 \quad (42)$$

with respect to λ .

Using the above equations, let us investigate static stability of 3-link serial chain using the developed matrix criterion in the S- and Z- configurations (these shapes of the chain correspond to the unloaded configurations). For the Z-configuration the unloaded configuration is defined by the angles $q^0 = 9.90^\circ$, $\theta_1^0 = -30^\circ$ and $\theta_2^0 = 30^\circ$ that correspond to the end point location $x = 2.91l$; $y = 0$. Modeling results are presented in Table I. This table includes the external loadings F that are normalized with respect to K_0 / L , the Cartesian stiffnesses K_C that are also normalized with respect to K_0 / L , and the static stability of serial chain configuration S_c (as it was mentioned negative value corresponds to stable configuration and positive to unstable configuration) as well as the shapes of the chains. The results have been obtained for the cases of $\Delta = 0$ and $\Delta = 0.2$, here Δ is the normalized the end-point deflection $\Delta = \delta / l$, and δ is the absolute displacement.

Table 1 Static stability of 3-link serial chain under loading

	S-configuration		Z-configuration	
	stable	unstable	stable	unstable
$\Delta = 0$				
Shape				
F	0.5	2	0	-3.05
K_C	Inf	Inf	16.93	0.53
S_c	-0.60	0.30	-0.67	1.33
$\Delta = 0.2$				
Shape				
F	-1.03	-3.11	-1.05	-3.03
K_C	0.18	0.57	0.21	0.81
S_c	-0.63	1.34	-0.35	1.26

The results show that for the stable configurations the value of S_c is always negative and for the unstable configurations it is positive. Hence, numerical results that have been obtained using the stability criterion (21) are in a good agreement with analytical ones. Moreover, it is shown that for the unstable configuration the stiffness coefficient K_C is positive and, consequently, it cannot be used for the static stability analysis of kinematic chain configuration.

5.2 Static stability of serial chain under auxiliary loading

Let us now focus on the static stability analysis of a serial chain under auxiliary loadings applied to an intermediate node. It is assumed that the considered chain consists of two rigid links separated by a flexible joint and two passive joints at both ends. It is assumed that the left passive joint is fixed with a physical constraint, while the right one is balanced by external loading F_x and can be moved along x direction (Figure 10). Besides, here both rigid links have the same length L and the actuator stiffness is K_0 .

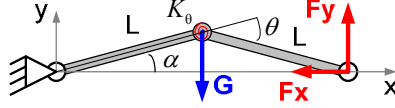


Figure 10 Kinematic chain with compliant actuator between two links and its static forces

Let us assume that the initial configuration (i.e. for $M_\theta = 0$) of the manipulator corresponds to $\theta_0 = -\pi/6$, where $\theta = -2\alpha$ is the coordinate of the actuated joint, α is the angle between the first link and x -direction. It is also assumed that the external loading G is applied to the intermediate nod (Figure 10) and it is required to apply the external loading (F_x, F_y) at the end-point to compensate the auxiliary loading G . Since this example is quite simple, it is possible to obtain the force-deflection relation and the stiffness coefficient analytically. The force-displacement relation and the stiffness K_x can be expressed in a parametric form as

$$F_x = -\frac{G \cos \alpha}{2 \sin \alpha} - 2 \frac{K_0 \cdot (\alpha - \alpha_0)}{L \sin \alpha}; \quad F_y = -\frac{G}{2} \quad (43)$$

$$K_x = -\frac{G}{4L \sin^3 \alpha} - \frac{K_0 \cdot (\alpha - \alpha_0) \cos \alpha - \sin \alpha}{L^2 \sin^3 \alpha}; \quad K_y = 0 \quad (44)$$

where $\alpha \in (-\pi/2; \pi/2)$ is treated as a parameter, parameter α_0 defines an initial configuration of serial chain (i.e. before applying the external force (F_x, F_y)).

As it follows from expression (44), the stiffness coefficient K_x essentially depends on the auxiliary loading G , coefficient K_x can be both positive and negative or even equal to zero when the auxiliary loading is equal to its critical value $G^* = 4K_0 / L \cdot \sin \alpha_0$. It is evident that the case $G > G^*$ is very dangerous from practical point of view, since the chain configuration is unstable.

The force-deflection relations and values of translational stiffness K_x are presented in Figure 11. They show that the auxiliary loading G significantly reduces the stiffness of the serial chain. Further increasing of the auxiliary loading up to $G = 1.5 \cdot G^*$ leads to the unstable configuration with negative stiffness $-7.46 \cdot K_0 / L^2$.

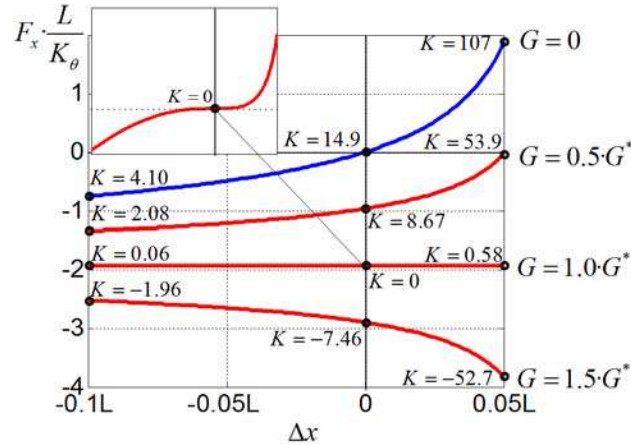


Figure 11 Force-deflections relations for different values of auxiliary loading G ($G^* = 4K_0 / L \cdot \sin \alpha_0$, $K_x = K \cdot K_0 / L^2$)

To investigate the static stability of serial chain configuration and the static stability of the end-point location additional, analysis have been performed. Simulation results are summarized in Table II that contains both translational stiffness $K = K_x \cdot L^2 / K_0$ and stability coefficients δW for different values of auxiliary loading G and displacements Δx . The results confirm that when auxiliary loading G overcomes its critical value G^* both configuration and the end-point location of serial chain become unstable. Hence, the presented case study demonstrates rather interesting features of stiffness behavior for kinematic chains under auxiliary loading that were not studied before (negative stiffness, non-monotonic force-deflection curves, etc.).

Table 2 Translational stiffness $K = K_x \cdot L^2 / K_\theta$ and stability coefficients S_c for different values of auxiliary loading G and different displacements Δx ($G^* = 4K_\theta / L \cdot \sin \alpha_0$)

G	Performance measures	$\Delta x = -0.05L$	$\Delta x = 0$	$\Delta x = 0.05L$
0	K	6.69	14.9	107
	S_c	-0.50	-0.66	-1.29
$0.5 \cdot G^*$	K	3.36	8.67	53.9
	S_c	-0.28	-0.35	-0.66
$1.0 \cdot G^*$	K	0.03	0	0.58
	S_c	-0.06	-0.04	-0.03
$1.5 \cdot G^*$	K	-3.31	-7.46	-52.7
	S_c	0.16	0.26	0.60

5.3 Kinetostatic singularity in the neighborhood of the flat configuration

Let us consider now an example that deals with the static stability analysis of Orthoglide manipulator (Figure 12a). Detailed specification of this manipulator can be found in Chablat (2003), some results on the stiffness analysis have been presented in Pashkevich (2010, 2011), its elastostatic parameters have been summarised in Klimchik (2013). In this case study let us address the stiffness analysis (which includes static stability analysis of end-point location under external loading) of Orthoglide manipulator in the neighborhood of a flat configuration. Simulation results for this posture are presented in (Figure 12b and Table III where d_0 denotes the initial distance from the flat singularity, K_0 is the translational stiffness for the unloaded mode, $(\Delta_{cr}^+, F_{cr}^+)$ and $(\Delta_{cr}^-, F_{cr}^-)$ are respectively the critical deflection and the critical force for the opposite directions of the displacement. As it follows from these results, in the neighborhood of the flat singularity the stiffness properties are essentially non-symmetrical with respect to the force direction. In particular, for the inside-direction of the loading, the force increases non-linearly but monotonically while the deflection augments. However, for the outside-direction, initially the manipulator reacts to the external loading in the same way: increasing of the deflection leads to increasing of the resisting elastic force. But after achieving the critical value, the reacting force begins decrease, the configuration becomes unstable and the manipulator abruptly changes its posture to the symmetrical ones. After that, the manipulator demonstrates stable behavior with respect to the loading.

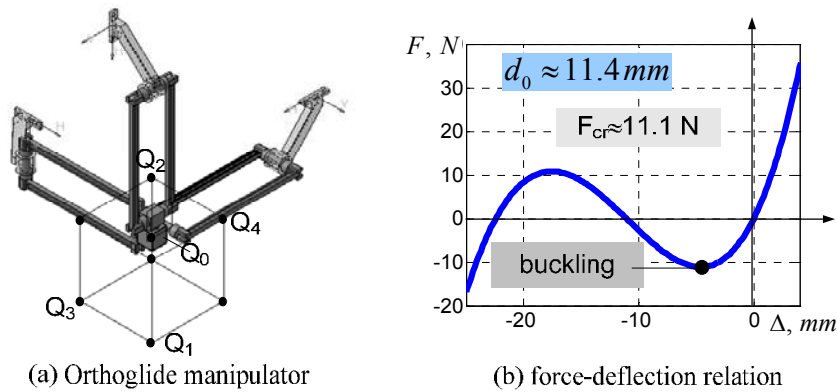


Figure 12 Force-displacement relations for Orthoglide manipulators (distance to the singularity is 11.4 mm)

The simplest model that explains the above described phenomenon is presented in Figure 13. It is derived via generalization of the “toggle-frame” construction, with relevant modifications motivated by the Orthoglide architecture and relative stiffness properties of its elements. Here, the elasticity is concentrated at the basis of the manipulator legs and it is presented by linear springs with the parameter K_θ . It is assumed that initial distance between the end-point and the singularity-plane is $d_0 = L \sin \varphi_0$, where φ_0 is corresponding angle between the leg and the plane. The derived expressions

Static stability of manipulator configuration: influence of the external loading.

$$\begin{aligned} F &= 3K_\theta L_0 (1 - \cos \varphi_0 / \cos \varphi) \sin \varphi; \\ \Delta d &= L_0 (\sin \varphi_0 - \sin \varphi) \end{aligned} \quad (45)$$

perfectly describe the shape of the force-deflection curves obtained from the complete stiffness models. Here, parameter Δd defines the displacement of the end-effector.

Table 3 Summary of stiffness analysis in the neighborhood of the flat singularity

Configuration	d_0 , [mm]	F_{cr}^- , [kN]	Δ_{cr}^- , [mm]	F_{cr}^+ , [kN]	Δ_{cr}^+ , [mm]
Point Q_2	91.7	-2.06	-5.7	2.20	4.9
Point Q_2^a	46.0	-0.70	-17.1	1.45	11
Point Q_2^b	11.4	-0.01	-4.6	0.92	24

$Q_2 = (-76.35, -76.35, -76.35)$; $Q_2^a = (-100, -100, -100)$; $Q_2^b = (-120, -120, -120)$

Besides, more detailed analysis shows extremely fast reduction of the stiffness while approaching this singularity. Corresponding expressions derived for small value of φ_0 yield a linear relation for the critical deflection $\Delta_{cr} \approx 0.42d_0$ and cubic relation for the critical force $F_{cr} \approx K_\theta / \sqrt{3}L^2 \cdot d_0^3$. Hence, this simplified model is in good agreement with the simulation results and justifies conventional kinematic design objectives (velocity transmission factors, condition number, etc.) that preserve the manipulator from approaching the flat posture.

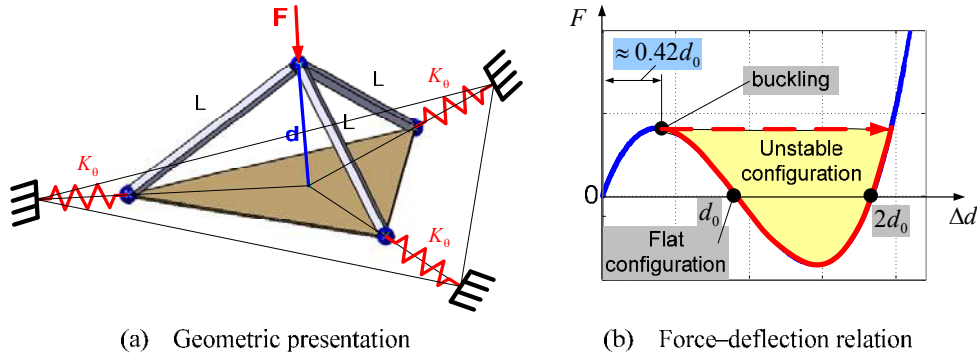


Figure 13 Simplified stiffness model of Orthoglide-type manipulators for near-flat configuration

Hence, the considered example illustrates the ability of proposed technique to obtain the full-scale force-deflection relation for the parallel manipulators that is suitable for the static stability analysis of end-point location under the external loading. It proves that the common notion of the “distance-to-singularity” that is used in kinematics must be revised in elastostatics taking into account that loading essentially reduces the margin of the manipulator structural stability.

6 Conclusion

The paper presents new approach for the static stability analysis of parallel manipulators under internal and external loadings applied to different points. In contrast to other works, it is proposed to address both static stability of the end-effector location and static stability of kinematic chain configuration. This approach is based on the non-linear stiffness analysis that includes computing the static equilibrium configuration corresponding to the given loadings as well as computing the Cartesian stiffness matrices for serial chains and parallel manipulators. The advantages of the proposed approach are illustrated by several examples

7 Acknowledgment

The work presented in this paper was partially funded by the Region “Pays de la Loire”, France, by the project ANR COROUSSO, France and FEDER ROBOTEX, France.

8 References

- Alici, G., Shirinzadeh, B. 2005. Enhanced stiffness modeling, identification and characterization for robot manipulators. *IEEE Transactions on Robotics* 21(4), 554–564.
- Angeles, J. 2007. *Fundamentals of Robotic Mechanical Systems: Theory, Methods, and Algorithms*, Springer, New York, 2007.
- Chablat, D., Wenger, P. 2003. Architecture Optimization of a 3-DOF Parallel Mechanism for Machining Applications, the Orthoglide. *IEEE Transactions On Robotics and Automation* 19(3), 403-410.
- Chakarov D. 2004. Study of antagonistic stiffness of parallel manipulators with actuation redundancy. *Mechanism and Machine Theory* 39, 583–601.
- Chen, Sh.-F., Kao, I., 2002. Geometrical Approach to The Conservative Congruence Transformation (CCT) for Robotic Stiffness Control," *Proceedings of ICRA, 2002*, pp 544-549.
- Corradini, C., Fauroux, J.C., Krut, S., Company, O. 2004. Evaluation of a 4 degree of freedom parallel manipulator stiffness. in *Proceedings of the 11th World Cong. in Mechanism & Machine Science (IFTOMM'2004)*, pp. 1857-1861.
- Deblaise, D., Hernot, X., Maurine, P. 2006. A systematic analytical method for PKM stiffness matrix calculation. *Proceedings of ICRA conference 2006*, pp. 4213-4219.
- Dumas, C., Caro, S., Cherif, M., Garnier, S., Furet, B. 2010. A Methodology for Joint Stiffness Identification of Serial Robots. in *Proceedings of the International Conference on Intelligent Robots and Systems (IROS 2010)*, pp. 464 - 469.
- Gantmacher F. 1959. *Theory of matrices*. AMS Chelsea, 1959
- Gosselin, C. 1990. Stiffness mapping for parallel manipulators. *IEEE Transactions on Robotics and Automation* 6(3), 377–382.
- Klimchik, A., Pashkevich, A., Caro, S., Chablat, D. 2012. Stiffness matrix of manipulators with passive joints: computational aspects. *IEEE Transactions on Robotics* 28(4), 955-958
- Klimchik, A., Pashkevich, A., Chablat, D. 2013. CAD-based approach for identification of elasto-static parameters of robotic manipulators. *Finite Elements in Analysis and Design* 75, 19–30
- Kövecses, J., Angeles, J. 2007. The stiffness matrix in elastically articulated rigid-body systems. *Multibody System Dynamics*, 169–184.
- Merlet J.-P. 2008. *Parallel Robots*. 2nd Edition, Springer, 2008.
- Pashkevich, A., Chablat, D., Wenger, P. 2010. Stiffness analysis of overconstrained parallel manipulators. *Mechanism and Machine Theory* 44, 966-982.
- Pashkevich, A., Klimchik, A., Chablat, D. 2011. Enhanced stiffness modeling of manipulators with passive joints. *Mechanism and Machine Theory* 46(5), 662-679.
- Quenouelle, C., Gosselin, C.M. 2008. Stiffness Matrix of Compliant Parallel Mechanisms. In *Springer Advances in Robot Kinematics: Analysis and Design*, pp. 331-341.
- Salisbury, J. 1980. Active Stiffness Control of a Manipulator in Cartesian Coordinates. in *Proceedings of the 19th IEEE CDC conference 1980*, pp. 87–97.
- Shan, X., Menq, C.-H. 2002. Robust Disturbance Rejection for Improved Dynamic Stiffness of a Magnetic Suspension Stage. *IEEE/ASME transactions on mechatronics*. 7(3), 289-295
- Su, Y.X., Duan, B.Y., Nan, R.D., Peng, B. 2003. Mechatronics Design of Stiffness Enhancement of the Feed Supporting System for the Square-Kilometer Array. *IEEE/ASME transactions on mechatronics* 8(4), 425-430
- Tyapin, I. Hovland, G. 2009. Kinematic and elastostatic design optimization of the 3-DOF Gantry-Tau parallel kinematic manipulator. *Modelling, Identification and Control* 30(2), 39-56
- Wei, W., Simaan, N. 2010. Design of planar parallel robots with preloaded flexures for guaranteed backlash prevention, *Journal of Mechanisms and Robotics* 2(1), 10 pages.
- Xi, F., Zhang,, D., Mechefske, Ch.M., Lang, Sh.Y.T. 2004. Global kinetostatic modelling of tripod-based parallel kinematic machine. *Mechanism and Machine Theory* 39, 357–377.
- Yi, B.-J., Freeman, R.A. 1993. Geometric analysis antagonistic stiffness redundantly actuated parallel mechanism. *Journal of Robotic Systems* 10(5), 581-603.